Compact Wideband SIW Based Bandpass Filter for X, Ku and K Band Applications

Tharani DURAISAMY [1], Selvajyothi KAMAKSHY [1],Sholampettai Subramanian KARTHIKEYAN [2], Rusan Kumar BARIK [3], Qingsha S. CHENG [3]

[1]Dept. of Electronics and Communication Engineering, Indian Institute of Information Technology Design & Manufacturing (IIITDM) Kancheepuram, Chennai-600127, India
[2]Dept. of Electronics and Communication Engineering, National Institute of Technology, Tiruchirappalli, Tamil Nadu-620015, India
[3]Dept. of Electrical and Electronic Engineering, Southern University of Science and Technology, Shenzhen, China

{edm17d009, ksjyothi}@iiitdm.ac.in, sskarthikeyan@nitt.edu{rusanbarik, chengqs}@sustech.edu.cn

Submitted September 29, 2020 / Accepted March 23, 2021

Abstract. *This paper presents a miniaturized bandpass filter (BPF) with characteristics of wider passband and stopband rejection using substrate integrated waveguide (SIW) technology. Slot loading mechanisms deployed on the upper layer of SIW and defective ground structure (DGS) on the ground plane are utilized to achieve wider passband and stopband respectively. The slots on the top layer along with DGS significantly enhances the selectivity of the filter by generating three transmission zeros (TZs) on the upper side of the passband. The proposed filter is simulated using full-wave simulators and the performance is validated through fabrication and testing of the prototype. The proposed SIW filter exhibits a low insertion loss of 1.52 dB over a wider passband from 9.17 GHz to 20.31 GHz with a 3 dB fractional bandwidth (FBW) of 76%. Further, a wider upper stopband is achieved with the rejection of more than 16 dB in the frequency range of 23 GHz to 40 GHz. The filter provides a flat group delay response of approximately 0.19 ns over the wider passband. The electrical size of the fabricated prototype is $1.05\lambda_g \times 0.67\lambda_g$, where λ_g denotes the guided wavelength in the dielectric substrate for the designed center frequency of 16 GHz.*

Keywords

Substrate integrated waveguide, band pass filter, compact, transmission zero, bow-tie shaped slot

1. Introduction

Recent developments in wireless communication systems demand the requirement of a Bandpass filter (BPF) with compact size, wideband, low insertion loss, high selectivity and wide out of band rejection. Substrate integrated waveguide (SIW) is a suitable technology to design BPF which yields the benefits of both the microstrip and rectangular waveguides. This enables to attain a cost effective solution, reducing losses, increasing the Q (quality) factor and power handling capacity, providing ease of integration with other planar components in the microwave communication system [1]. Microstrip BPF is implemented by combining low pass filter and high pass filter using the low pass to bandpass transformation, insertion loss (IL) technique or by employing multiple resonators. In [2], [3] the authors have designed a via less compact BPF using metamaterials (MTMs) to obtain large fractional bandwidth (FBW) and small insertion loss (IL). The resonant frequency is attained through split circular rings and rectangular stub in [2] and composite right-left handed transmission line (CRLH-TL) in [3] respectively.

Several SIW based filters were existing in the literature for realizing compact BPF with enhanced performance. BPFs are developed in SIW technology by using coupling resonators or introducing low pass structures such as electromagnetic bandgap (EBG) structures into SIW high pass structures, MTMs, multimode resonators (MMRs) etc. MTMs are used in the design of SIW filters to achieve miniaturization and enhanced selectivity as in [4], [5]. EBG structures are incorporated in SIW to design millimeter-wave [6] and super-wide [7] BPF with merits of wide out of band rejection (OBR). EBGs along with folded SIW (FSIW) [8] and half-mode T septum SIW (HMTSSIW) [9] are used to achieve a significant size-reduction and larger bandwidth but sacrificing the requisite of low IL. Quasi-elliptic filters are designed using SIW by utilizing slot-coupling [10] and cross coupling [11] with benefits of low IL.

Different coupling topologies such as source-load coupling [12], cascaded trisection [13], stepped impedance non-resonating node (NRN) [14], modified feeding and coupling [15], mixed electric and magnetic coupling [16], negative coupling [17] and magnetic coupling [18] are used in

the design of SIW BPF. These topologies achieve high selectivity, but with the demerits of high IL [12], [15] due to their inverse relationship between bandwidth and has a larger circuit size [12,13,15]. SIW BPF is realized using planar resonators suitable for System-on-package (SoP) [19], where it lacks selectivity at the upper side of the passband. A compact SIW BPF useful for millimeter (mm) wave is demonstrated using 3-D ICs technology [20].

Compact wideband SIW filters are designed using MMRs such as U-shaped slots and comb-shaped slots together with defective ground structure (DGS) in [21], [22] respectively to gain good upper stop band performance. The non-fundamental mode is utilized in [23] to design a K-band SIW filter for enhancing stopband performance where a multilayered structure is deployed. Stepped impedance face-to-face E-shaped slots that act as DGS is employed to design SIW filter for the forthcoming 5G applications at the expense of large IL [24]. Multimode BPF such as triple mode filter [25] and quintuple mode filters [26] are designed using SIW and quarter mode SIW (QMSIW) structures respectively. They have improved out of band rejection in both the edges of pass bands. To achieve significant size reduction, QMSIW and Eighth Mode SIW (EMSIW) structures [27] are used to design balanced filters. Most of the SIW filters reported in in the literature [12–15, 19, 23–25] suffer from narrow FBW, high IL and larger circuit size. As global technology progresses towards miniaturization, the requirement for wideband filters with a smaller footprint, small insertion loss and good selectivity has gained much interest among the researchers.

In this paper, the SIW bandpass filter with enhanced performance useful for X, Ku and K band applications is proposed.

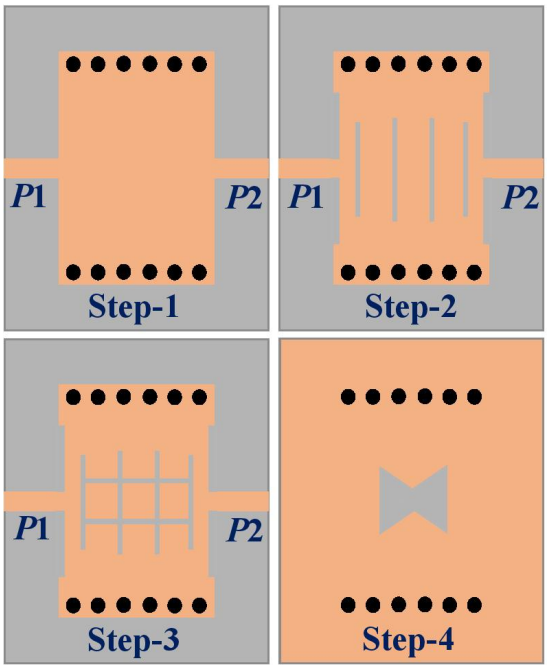

Fig. 1. Design evolution of the proposed SIW WBBPF.

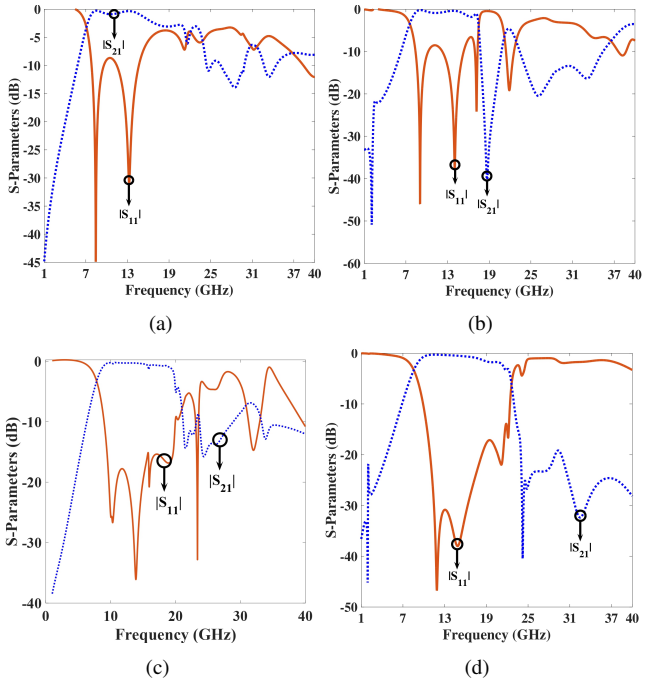

Fig. 2. Simulated S-parameters of the SIW filter structure corresponding to (a) Step 1, (b) Step 2, (c) Step 3 and, (d) Step 4.

The wider passband is generated due to multimode resonance by a combination of longitudinal and transverse slots engraved on the top layer of SIW. Band rejection characteristics of bowtie-shaped DGS improves the stopband performance and further due to the combined action of slots and DGS the selectivity of the proposed filter is enhanced by creating 3 TZs. The size-reduction of the designed filter is attributed to the loading of multiple slots that eventually leads to an increase in electrical length. For validation purposes, the filter prototype has been fabricated and good agreement is achieved between the simulated and measured results. The key features of the proposed work are:

- The size of the proposed SIW based wideband filter is highly miniaturized than the previously reported filters [6, 7, 9, 11–16, 19, 21–26].
- Compared to the existing filters, the proposed filter structure has low IL [4, 7–10, 12–15, 19, 23–26], better return loss [2, 4, 6–9, 12–16, 20–22, 24–26] and wider FBW [2, 4–7, 10–27].
- The proposed wideband filter provides wider stopband rejection and flat group delay response.
- To investigate the multimode resonant behavior of the slot-loaded filter, the variation of input impedance w.r.t the number of slots is analyzed.
- Parametric analysis is explored to verify the dependence of the filter performance on the slot dimensions, their position and bowtie-shaped DGS dimensions.

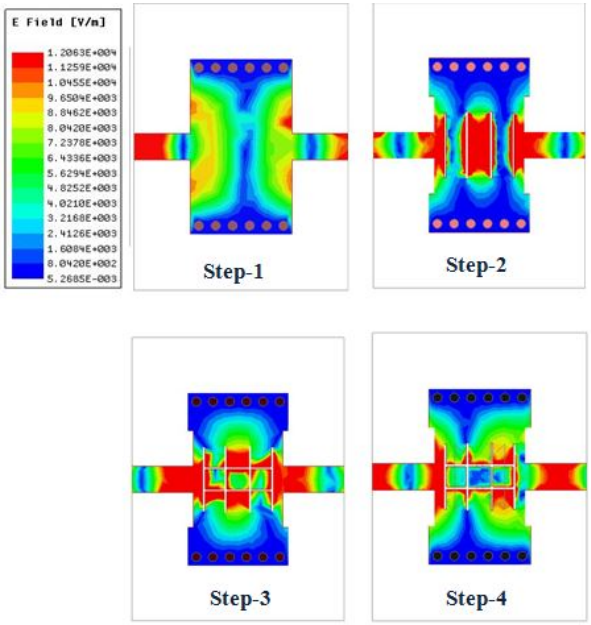

Fig. 3. Simulated electric field distribution of the proposed filter at designed center frequency of 16 GHz.

The rest of the paper is organized as follows. Section 2 elaborates the design evolution of the proposed filter configuration along with parametric study. Section 3 shows the fabrication and experimental validation of the proposed filter and finally, Section 4 presents the conclusions.

2. Design of Wideband SIW Bandpass Filter

The design of the proposed SIW wideband bandpass filter (WBBPF) is based on the evolution of steps that are illustrated in Fig. 1 along with its corresponding simulated S-parameters in Fig. 2. The design procedure is as follows:

- In step-1, a conventional SIW filter is constructed using a rectangular SIW cavity by following the design equations in [1].
- Multimode resonance is created utilizing transverse slots in the top layer of the SIW filter as illustrated in step-2.
- In step-3, in-band return loss performance is enhanced by incorporating longitudinal slots together in cross-Section with transverse slots. The size-reduction of the proposed filter is contributed by the loading of multiple slots.
- Finally, stopband characteristics of the filter is improved by employing bowtie-shaped DGS in the ground plane as step-4.

The basic structure of the proposed filter consists of a rectangular SIW cavity that is fed by two 50 Ω microstrip lines. To ensure confinement of the electric field inside SIW, the pitch of the via-holes is chosen less than or equal to twice its diameter. The SIW filter depicted in step-1 of Fig. 1 exhibit high pass characteristics as shown in Fig. 2(a) whose cut-off frequency is in coincidence with the calculated cut-off frequency of SIW [1]. This filter structure exhibits TE_{101} electric field distribution which is the dominant mode as shown in step-1 of Fig. 3. The following equation is used to compute the resonant frequency of the dominant mode of SIW cavity:

$$f_{c(TE_{101})} = \frac{1}{2\pi\sqrt{\mu\varepsilon}}\sqrt{\left(\frac{m\pi}{L_{\text{eff}}}\right)^2 + \left(\frac{n\pi}{W_{\text{eff}}}\right)^2} \tag{1}$$

where $m = 1, 2,..., n = 1, 2,...,$ ε and μ denotes the permitivitty and permeability of the substrate. The effective length and width of the cavity are determined using:

$$\begin{aligned} L_{\text{eff}} &= L - 1.08\frac{d^2}{s} + 0.1\frac{d^2}{L_{\text{s}}}, \\ W_{\text{eff}} &= W - 1.08\frac{d^2}{s} + 0.1\frac{d^2}{W_{\text{s}}} \end{aligned} \tag{2}$$

where W_{s} and L_{s} are specified as width and length of the cavity. The diameter and the center-to-center spacing between the via-holes are denoted by d and s, respectively. To meet the constraint of minimum leakage loss, the diameter and pitch need to be chosen as $d/\lambda_{\text{g}} \leq 0.1$ and $d/s \geq 0.5$ (λ_{g} denotes the guided wavelength at the resonating frequency).

2.1 The Impact of Transverse and Longitudinal Slots

To enable bandpass filtering, periodically spaced four transverse slots of length W_{c} and $W_{\text{d}} < \lambda_{\text{g}}/2$ (where f = 16 GHz) is etched from the top metallic layer of SIW. The slot-loading mechanism modifies the resonant mode of rectangular SIW since the slots are oriented in such a way to cut the current lines of unperturbed mode. Hence higher-order mode TE_{201} gets excited that creates additional resonance as illustrated in step-2 of Fig. 3. The gap between the adjacent slots is assumed to be equal and considered as $L_{\text{b}} = W_{\text{b}} = 0.58\lambda_{\text{g}}$. These slots create a wider passband from 7.66 GHz to 17.54 GHz due to multimode resonance in spite of poor return loss performance in passband as shown in Fig. 2(b).

Two longitudinal slots of length $L_{\text{t}} = \lambda_{\text{g}}/2$ separated by a distance of $W_{\text{b}} = 0.58\lambda_{\text{g}}$ are etched from the top layer of the SIW filter. These slots create additional resonance due to perturbation of TE_{101} mode that significantly improves in-band filtering especially the return loss performance within the passband as depicted in Fig. 2(c).

2.2 Band Rejection Property of DGS

To achieve better stopband performance, bowtie-shaped DGS with $L_{\text{e}} = 0.36\lambda_{\text{g}}$ and $W_{\text{e}} = 0.47\lambda_{\text{g}}$ is incorporated in the middle of the ground layer as shown in step-4 of Fig. 1. After incorporating the DGS in the filter structure, the passband frequency is shifted from 8.96 GHz to 10.03 GHz due

to the change in effective inductance and capacitance of the DGS. It is noticed that the bandwidth of the filter is widened from 11 GHz (8.96 to 19.96 GHz) to 12.43 GHz (10.03 to 22.4 GHz) because of the increased fringing field resulting in parasitic capacitance created by the DGS. This capacitance strengthens the coupling between the top and bottom metallic layer resulting in an improved bandwidth [22].

The schematic of the proposed wideband SIW BPF is depicted in Fig. 4. The physical parameters of the proposed filter are optimized to achieve the desired frequency response using the full-wave simulator and the final optimized dimensions of the proposed WBBPF are given in Tab. 1. Simulation results shown in Fig. 5 reveals that the proposed filter exhibits a low insertion loss of 0.64 dB with a 3 dB FBW of 89 % and a return loss of more than 17 dB. Stopband rejection at 24.22 GHz is found to be 44.13 dB with a wideout of band rejection of greater than 19.4 dB from 23 GHz to 40 GHz. The band stop behavior of DGS suppresses the higher-order harmonics thereby wide stopband is made possible. It can be seen from Fig. 6, group delay is approximately 0.19 ns over the entire desired passband.

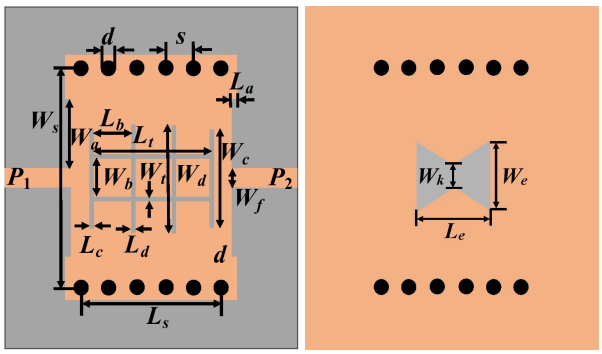

(a) (b)

Fig. 4. Schematic of the proposed wideband SIW BPF (a) Top view, (b) Bottom view (grey-substrate, orange-copper).

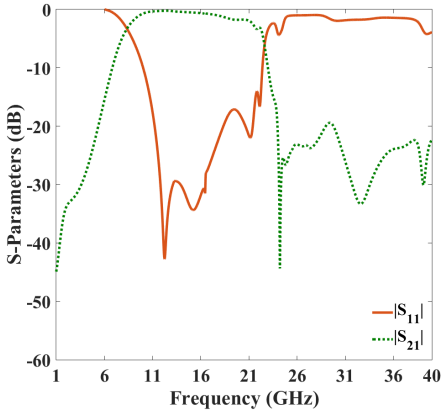

Fig. 5. Simulated scattering parameters of the proposed WBBPF.

W_s	14	W_a	3.2	W_c	5.8	W_t	0.2
L_s	9.0	L_a	0.5	L_c	0.2	L_t	6.3
d	0.8	W_b	1.8	W_d	6.0	s	1.5
L_b	1.8	L_d	0.2	W_e	5.83	L_e	4.44
W_k	1.52	W_f	2.31				

Tab. 1. Dimensions of the proposed SIW WBBPF (in mm).

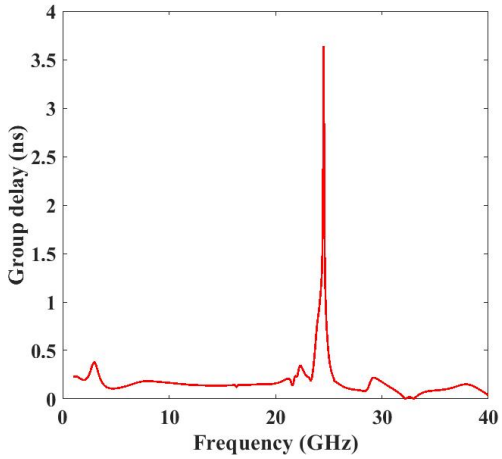

Fig. 6. Simulated group delay response of the proposed WBBPF.

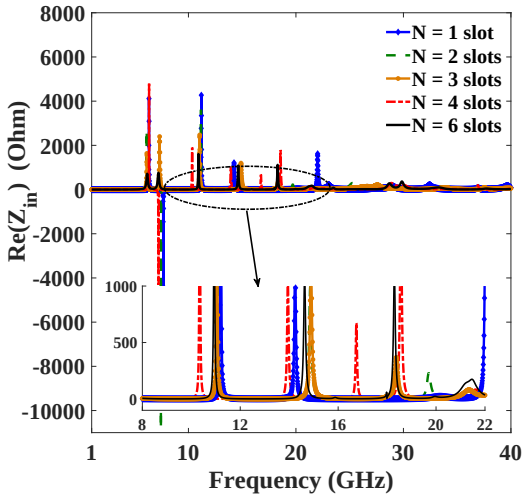

Fig. 7. Input impedance plot by varying the number of slots.

2.3 Parametric Analysis

A parametric study is carried out to investigate the effect of filter parameters on the performance of the proposed filter. The number of slots and their position determines the bandwidth of the filter. From Fig. 7, it is clear that as the number of transverse slots increases, significant variation is observed in the resonant modes of the filter in the upper X-band, Ku-band and lower K- band. The slots yield impedance matching between the closely occurring resonance in X-band, Ku-band and K-band, due to which wideband is achieved.

From Fig. 8, it is observed that as the number of transverse slots is increased from 1 to 2, the bandwidth of the filter increases affecting the return loss (RL). Further, the addition of two more transverse slots, reduces the bandwidth; due to the excitation of higher-order modes. However, the desired bandwidth is obtained by the addition of two more longitudinal slots resulting in 6 slots. The effect of the position of slots on the in-band return loss performance of the proposed filter is depicted in Fig. 9. It can be seen that better return loss is

achieved in the desired passband for the case where the transverse slots are placed at a spacing of L_b = 1.8 mm. Hence maximum of four transverse slots can be accommodated on the longitudinal slot of length L_t = 6.3 mm.

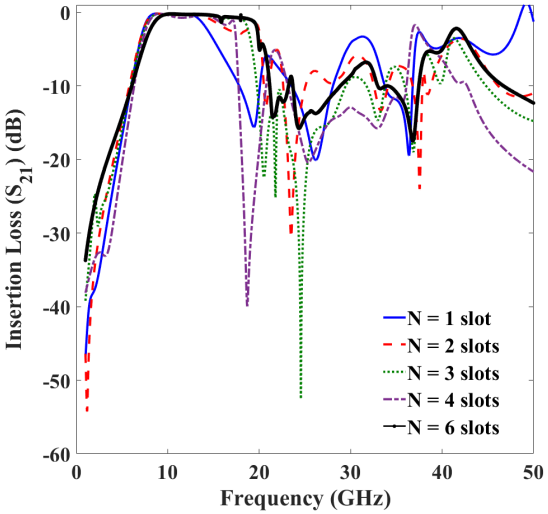

Fig. 8. Simulated transmission response by varying the number of slots.

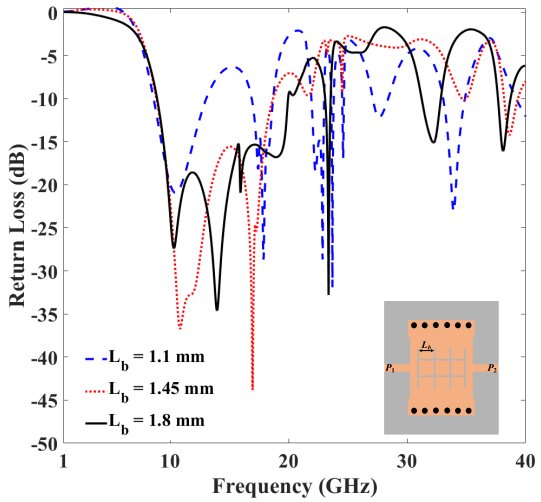

Fig. 9. Simulated return loss (S_{11}) of the proposed filter (Step-3).

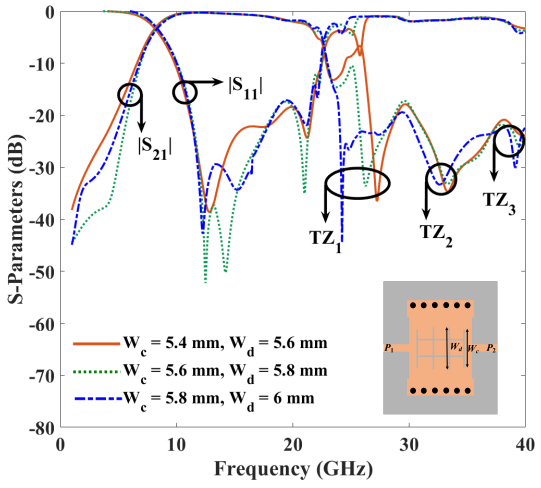

Fig. 10. Simulated S-parameters of the proposed filter against varied stub length W_c and W_d.

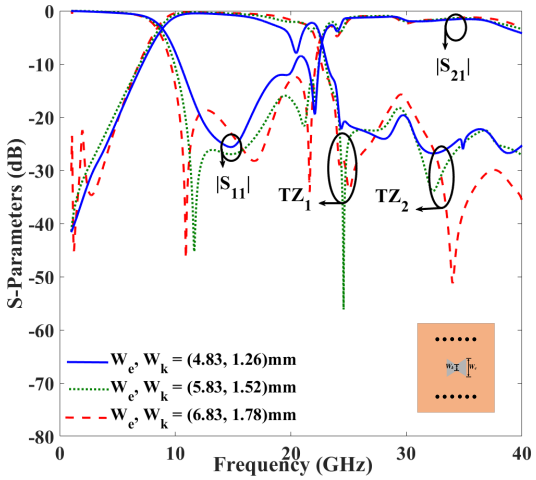

Fig. 11. Simulated S-parameters of the proposed wideband SIW BPF with variation of width of bow-tie shaped slot.

The slots on the upper metallic layer of the SIW filter acts as an open stub. The transmission zeros (TZs) are generated by the combined effect of slots on the upper layer of SIW and DGS incorporated on the bottom layer of SIW. The location of TZ basically depends on the length of the stub (slot). As the stub lengths W_c and W_d are increased from 5.4 mm to 5.8 mm and 5.6 mm to 6 mm respectively, return loss values slightly increases within the passband, though TZ_1 location moves downwards towards the lower frequency side, there is a small effect on TZ_2 location and no effect on TZ_3 location that can be observed from Fig. 10. Since the length of stub affects the electrical length and finally impedance of stub which affects the frequency at which TZ occurs [22]. For W_c = 5.8 mm and W_d = 6 mm, there is a sharp transition from passband to stopband. As the width of the slots is increased, no significant influence is observed in the filter response. Also, to confirm that the important transmission zero is not created by the DGS itself a study is performed by varying the dimensions of DGS as illustrated through Fig. 11. It is clear that TZ_1 is unperturbed even if the DGS dimensions are varied.

The effect of bow-tie-shaped DGS in the ground plane is analyzed by altering the width of bow W_e from 4.83 mm to 6.83 mm that simultaneously alters the parameter W_k from 1.26 mm to 1.78 mm. As the width is increased, the lower and upper band edge frequencies shift towards lower frequencies due to an increase in capacitive loading which can be clearly seen from the S-parameter response shown in Fig. 11.

Actually the width of SIW determines the higher cutoff frequency and the parameters such as dimensions of slots determines the position of TZ_1, the spacing between the adjacent slots have an effect on in-band return loss and the number of slots determines the desired bandwidth range of the proposed filter. On the other hand, DGS enhances the stopband performance of the filter by enhancing the stopband rejection.

Ref.	Filter Type	CF [GHz]	3-dB FBW [%]	RL [dB]	IL [dB]	UBR [GHz]	TZs	Size [λ_g^2]
[2]	compact via-less	3.25	74.28	>15	0.6	5.32–6.88	2	0.0264
[3]	via-less	7.9	90	>20	0.5	-	2	0.425
[4]	FPD	1.54	5.8	>13	4	1.92–4.74	2	0.0112
[5]	FOCSRR	2.4	10.5	21	1.45	2.6–6	2	0.1209
[6]	mmWave	40	10.2	>13	1.42	45–50	3	6.56
[7]	Super wide	12.5	61.5	>10	<1.55	16.5–20	-	1.82
[8]	Folded SIW	5.7	77.2	>10	<2	-	-	0.7
[9]	Ultra wideband	6.8	115	>9.5	<2.5	11–13.6	-	1.32
[10]	Quasi-elliptic	3.7	16	>18	1.1	4–5	1	-
[11]	Quasi elliptic	10	1	NA	0.8	10.4–14	2	3
[12]	Transversal	14.87	1.5	14.3	3.9	15.2–18	2	4.6
[13]	TriSection	9	5.5	12	2.1	9.6–12	3	3.22
[14]	Inline	28	3.6	16	2.2	29.5–39	2	1.45
[15]	Narrow band	8.25	1.1	15	3.3	8.25–10.5	3	4
[16]	Cross coupled	10.13	10.8	17	1.5	11.2–13	3	1.555
[17]	High selectivity	1.528	11. 4	20	0.62	1.7–8	2	NA
[19]	SoP	5.1	4.2	>18	2.05	5.5–6	2	1.52
[20]	3D-IC	159.67	12.5	10	1.5	170–200	-	-
[21]	U-slot	8.5	42	11	1.1	11–18.5	1	0.7875
[22]	Wideband	13	48	>14	1.1	16.5–20	3	1.537
[23]	K- band	22.2	1.44	30	2.9	22.8–30	-	3.44
[24]	5G	38.2	8.4	>12	1.7	16.5–20	3	2.75
[25]	Triple mode	-	15.7	>15	1.8	7.5–10	3	-
[26]	Quintuple W-band	8.9	22.5	>15	1.97	115–125	4	1.56
[27]	EMSIW	3.09	15.2	>15	1.34	3.5–8	2	0.29
This Work	**Slots with DGS**	**14.74**	**76**	**>17.6**	**<1.5**	**23 - 40**	**3**	**0.7035**

Tab. 2. Performance comparison between reported and proposed SIW BPF. (CF: Center frequency; FBW: Fractional bandwidth; RL: Return loss; IL: Insertion loss; UBR: upper-band rejection; TZ: Transmission zeros).

3. Fabrication and Measurement

The proposed wideband SIW BPF is fabricated using 0.787 mm thick Rogers RT/Duroid 5870 substrate material having a relative permittivity ϵ_r = 2.33 and loss tangent tanδ = 0.0012. Figure 12 shows the photograph of the fabricated prototype. The size of the proposed filter excluding the feeding lines is 15.5 mm × 9 mm.

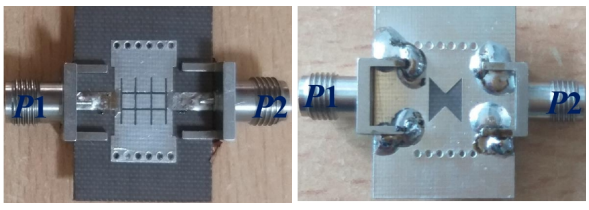

(a) (b)

Fig. 12. Fabricated prototype (a) Top view, (b) Bottom view.

In order to study the performance of the fabricated filter, the input and output ports are provided via SMA F edge mount (40 GHz) connectors. Transmission and reflection characteristics of the fabricated prototype are measured using Anritsu MS46122B (43.5 GHz) vector network analyzer (VNA). Figure 13. plots the comparison of S-parameters of the fabricated filter obtained from simulations and measurements. The fabricated filter has a wider passband ranging from 9.17 GHz to 20.31 GHz with a 3-dB fractional bandwidth of 76 %. The filter has a measured insertion loss of 1.52 dB within passband and return loss of more than 17.6 dB. Transmission zero (TZ_1) location is shifted towards a higher frequency of 25.68 GHz with 44.4 dB rejection. In addition to this, the proposed filter achieves a wider upper stopband having an attenuation of 16 dB up to 40 GHz. Measured results match very well with those obtained from simulation, except for the slight discrepancies owing to connector loss and fabrication tolerances. Table 2 gives a comparison between the proposed wideband SIW filter and other reported works in literature.

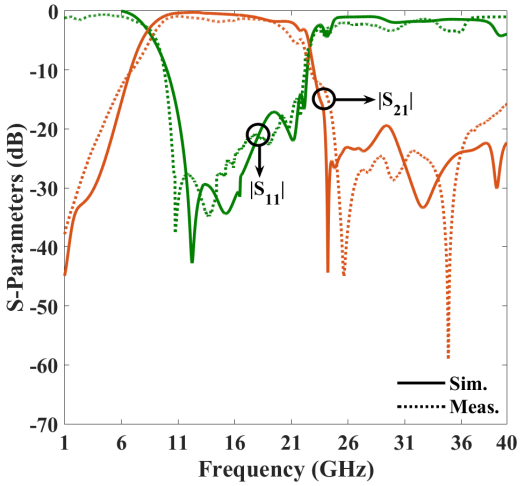

Fig. 13. Simulated and measured S-parameters of proposed wideband SIW BPF.

It is evident that the proposed filter has a larger 3 dB FBW than those reported in literature except in wideband SIW BPF proposed in [3], [8] and [9], where the filter design is complicated. The proposed filter has a comparatively smaller size, reasonable IL and better stop band performance than other reported SIW filters.

4. Conclusions

In this paper, a miniaturized wideband SIW BPF suitable for RADAR and satellites operating in the X band, Ku band and K band is designed, fabricated and experimentally verified. Wider passband is generated due to multimode resonance of slots loaded on the top layer of SIW whereas, the bowtie-shaped DGS incorporated on the ground plane is responsible for wider stopband characteristics of the filter. Further, slots along with DGS enhances the selectivity of the filter by generating 3 TZs on the upper side of the passband. The impact of slot and DGS on the filter performance is analyzed by varying its physical parameters. Compact size with simple structure, low insertion loss, flat group delay response, wider passband and stopband are the desirable features of the proposed filter.

Acknowledgments

The authors express their deepest gratitude to Mr. Purushothaman and his team from Mini-Circuits, SEZ, Tambaram, Chennai for extending VNA support to measure the fabricated filter prototype.

References

[1] BOZZI, M., GEORGIADIS, A., WU, K. Review of substrate-integrated waveguide circuits and antennas. *IET Microwaves Antennas & Propagation*, 2011, vol. 5, no. 8, p. 909–920. DOI: 10.1049/iet-map.2010.0463

[2] CHOUDHARY, D. K., CHAUDHARY, R. K., A compact via-less metamaterial wideband bandpass filter using split circular rings and rectangular stub. *Progress In Electromagnetics Research Letters*, 2018, vol. 72, p. 99–106. DOI: 10.2528/PIERL17092503

[3] CHOUDHARY, D. K., CHAUDHARY, R. K., Vialess wideband bandpass filter using CRLH transmission line with semi-circular stub. In *International Conference on Microwave and Photonics (ICMAP)*, Dhanbad (India), 2015. DOI:10.1109/ICMAP.2015.7408758

[4] CHOUDHARY, D. K., CHAUDHARY, R. K., A compact SIW based filtering power divider with improved selectivity using CSRR. In*2017 Progress in Electromagnetics Research Symposium - Fall (PIERS - FALL)*, Singapore, 2017. DOI: 10.1109/PIERS-FALL.2017.8293337

[5] DANAEIAN, M., GHAYOUMI-ZADEH, H. Miniaturized substrate integrated waveguide filter using fractal open complementary split-ring resonators. *International Journal of RF and Microwave Computer Aided Engineering*, 2018, vol. 28, no. 5, p. 1–10. DOI: 10.1002/mmce.21249

[6] WONG, S. W., CHEN, R. S., WANG, K., et al. U-shape slots structure on substrate integrated waveguide for 40-GHz bandpass filter using LTCC technology. *IEEE Transactions on Components, Packaging and Manufacturing Technology*, 2015, vol. 5, no. 1, p. 128–134. DOI: 10.1109/TCPMT.2014.2367516

[7] HAO, Z. C., HONG, W., CHEN, J., et al. Compact super-wide bandpass substrate integrated waveguide (SIW) filters. *IEEE Transactions on Microwave Theory and Techniques*, 2005, vol. 53, no. 9, p. 2968–2977. DOI: 10.1109/TMTT.2005.854232

[8] GENG, L., CHE, W., DENG, K. Wideband bandpass filter of folded substrate-integrated waveguide integrating with stripline compact resonant cell. *Microwave Optical Technology Letters*, 2008, vol. 50, no. 2, p. 390–393. DOI: 10.1002/mop.23117

[9] WU, L. S., ZHOU, X. L., YI, W. Y. Ultra- wideband bandpass filter using half-mode T-septum substrate integrated waveguide with electromagnetic bandgap structures. *Microwave Optical Technology Letters*, 2009, vol. 51, no. 7, p. 1751–1755. DOI: 10.1002/mop.24404

[10] WONG, S. W., CHEN, R. S., LIN, J. Y., et al. Substrate integrated waveguide quasi-elliptic filter using slot-coupled and microstrip-line cross-coupled structures. *IEEE Transactions on Components, Packaging and Manufacturing Technology*, 2016, vol. 6, no. 12, p. 1881–1888. DOI: 10.1109/TCPMT.2016.2625744

[11] KIANI, S., REZAEI, P., KARAMI, M. Substrate integrated waveguide quasi-elliptic bandpass filter with parallel coupled microstrip resonator. *Electronic Letters*, 2018, vol. 54, no. 10, p. 667–668. DOI: 10.1049/el.2018.0170

[12] LI, R., TANG, X., XIAO, F. Design of substrate integrated wavgeuide transversal filter with high selectivity. *IEEE Microwave Wireless Component Letters*, 2010, vol. 20, no. 6, p. 328–330. DOI: 10.1109/LMWC.2010.2047518

[13] ZHANG, P. J., LI, M. Q. Cascaded triSection substrate-integrated waveguide filter with high selectivity. *Electronic Letters*, 2014, vol. 50, no. 23, p. 1717–1719. DOI: 10.1049/el.2014.3456

[14] HE, Z., YOU, C. J., LENG, S., et al. Compact inline substrate integrated waveguide filter with enhanced selectivity using new non-resonating node. *Electronic Letters*, 2016, vol. 52, no. 21, p. 1778–1780. DOI: 10.1049/el.2016.2712

[15] KHAN, A. A., MANDAL, M. K. Narrowband substrate integrated waveguide bandpass filter with high selectivity. *IEEE Microwave Wireless Component Letters*, 2018, vol. 28, no. 5, p. 416–418. DOI: 10.1109/LMWC.2018.2820605

[16] AZAD, A. R., JHARIYA, D. K., MOHAN, A. Substrate-integrated waveguide cross-coupled filters with mixed electric and magnetic coupling structure. *International of Journal Microwave and Wireless Technologies*, 2018, vol. 10, no. 8, p. 896–903. DOI: 10.1155/2013/682707

[17] HO, M. H., LEE, K. Y., CHEN, Y. C. Miniaturized bandpass filter design using substrate integrated waveguide cavities with enhanced signal selectivity. *Microwave Optical Technology Letters*, 2019, vol. 61, no. 5, p. 1185–1188. DOI: 10.1002/mop.31730

[18] ZHANG, H., KANG, W., WU, W. Miniaturized dual-band SIW filters using E-shaped slotlines with controllable center frequencies. *IEEE Microwave Wireless Component Letters*, 2018, vol. 28, no. 4, p. 311–313. DOI: 10.1109/LMWC.2018.2811251

[19] SHEN, W., YIN, W. Y., SUN, X. W., et al. Substrate-integrated waveguide bandpass filters with planar resonators for system-on-package. *IEEE Transactions on Components, Packaging and Manufacturing Technology*, 2012, vol. 3, no. 2, p. 253–261. DOI: 10.1109/TCPMT.2012.2224348

[20] LIU, X., ZHU, Z., LIU, Y., et al. Wideband substrate integrated waveguide bandpass filter based on 3-D ics. *IEEE Transactions on Components, Packaging and Manufacturing Technology*, 2019, vol. 9, no. 4, p. 728–735. DOI: 10.1109/TCPMT.2018.2878863

[21] CHEN, R. S., WONG, S. W., ZHU, L., et al. Wideband bandpass filter uisng U-slotted substrate integrated waveguide (SIW) cavities. *IEEE Microwave Wireless Component Letters*, 2014, vol. 25, no. 1, p. 1–3. DOI: 10.1109/IEEE-IWS.2015.7164522

[22] MUCHHAL, N., SRIVASTAVA, S. Design of wideband comb shape substrate integrated waveguide multimode resonator bandpass filter with high selectivity and improved upper stop band performance. *International of Journal RF and Microwave Computer Aided Engineering*, 2019, vol. 29, no. 9, p. 1–9. DOI: 10.1002/mmce.21807

[23] LEE, B., LEE, T. H., LEE, K., et al. K-band substrate-integrated waveguide resonator filter with suppressed higher-order mode. *IEEE Microwave Wireless Component Letters*, 2015, vol. 25, no. 6, p. 367–369. DOI: 10.1109/LMWC.2015.2421313

[24] LI, J., HUANG, Y., WANG, H., et al. 38 GHz SIW filter based on the stepped-impedance face-to-face E-shaped DGSs for 5G application. *Microwave Optical Technology Letters*, 2019, vol. 61, no. 6, p. 1500–1504. DOI: 10.1002/mop.31799

[25] LIU, Z., XIAO, G., ZHU, L. Triple-mode bandpass filters on CSRR-loaded substrate integrated waveguide cavities. *IEEE Transactions on Components, Packaging and Manufacturing Technology*, 2016, vol. 6, no. 7, p. 1099–1105. DOI: 10.1109/TCPMT.2016.2574562

[26] HUANG, X., L., ZHOU, L., YUAN, Y., et al. Quintuple-mode W-band packaged filter based on a modified quarter-mode substrate-integrated waveguide cavity. *IEEE Transactions on Components, Packaging and Manufacturing Technology*, 2019, vol. 9, no. 11, p. 2237–2247. DOI: 10.1109/TCPMT.2019.2925371

[27] LI, P., CHU, H., CHEN, R. S. Design of compact bandpass filters using quarter-mode and eighth-mode SIW cavities. *IEEE Transactions on Components, Packaging and Manufacturing Technology*, 2017, vol. 7, no. 6, p. 956–963. DOI: 10.1109/TCPMT.2017.2677958

About the Authors . . .

Tharani DURAISAMY received her B. E. degree in Electronics and Communication Engineering from J. J. College of Engineering and Technology Tiruchirappalli, India in 2010. She received her M.E. degree in Communication Systems from Saranathan College of Engineering, Tiruchirappalli, India in 2013. Currently, she is a Research Scholar with the department of Electronics and Communication Engineering in Indian Institute of Information Technology, Kancheepuram, India. Her research interest include microwave antenna, SIW passive components such power dividers, filters and diplexers. D. Tharani is a Student member of IEEE and IEEE MTT-S.

Selvajyothi KAMAKSHY studied at Thangal Kunju Musaliar College of Engineering, Kollam, India and received the B. T. degree (1995) in Electrical and Electronics Engineering from Kerala University, India. Received M.E degree (2004) in Power Electronics and Industrial Drives from Sathyabama Institute of Science and Technology, Chennai, India. She received Ph.D degree in Electrical Engineering from the Indian Institute of Technology, Madras in 2009. Currently, she is an Assistant Professor in Electrical Engineering, Indian Institute of Information Technology Design and Manufacturing, Kancheepuram, India. She has 20 years of teaching experience. Her areas of interest are Control and Instrumentation Engineering, Electric vehicles, Medical instrumentation, Power Electronics and control. Dr. Selvajyothi is a Life member of ISTE. She is a member of IEEE, IIIS and ESSI.

Sholampettai Submaranian KARTHIKEYAN received the Ph.D. degree from IIT Guwahati, India, in 2011. He has 13 years of educational activity and research experience in the area of RF and microwave. He was the Short-Term academic foreign visit U.K and France. He is currently Assistant Professor with the Department of Electronics and Communication Engineering, National Institute of Technology, Tiruchirappalli, India. He has authored or co-authored more than 100 scientific research papers and technical reports. His current research interests include microwave integrated circuits, biological effects of microwaves, computer-aided design of MICS, metamaterials/frequency selective surfaces (FSSs), fractal antennas, MIC antennas, metamaterial antennas, and substrate-integrated waveguides. Dr. Karthikeyan is a Chair of the IEEE-APS Society Madras chapter. He is a member of the IEEE, IEEE MTT-S, and IEEE AP-S. He is a Life Member of the ISTE.

Rusan Kumar BARIK received the B. T. degree in Electronics & Communication Engineering from Biju Patnaik University of Technology, Rourkela, India in 2012, M.Tech degree in Communication Systems Design and Ph.D. degree in Electronics Engineering from Indian Institute of Information Technology, Chennai, Tamil Nadu, India in 2015 and 2018, respectively. He joined the Department of Electronics and Communication Engineering, Christ University Bangalore, India, as an assistant professor in 2018. He is currently a Post-Doctoral Researcher with the Southern University of Science and Technology, Shenzhen, China. His research interests include multiband microwave passive devices, multiband antennas, and SIW components.

Qingsha S. CHENG received the B. E. and M. E. degrees from Chongqing University, Chongqing, China, in 1995 and 1998, respectively, and the Ph.D. degree from McMaster University, Hamilton, ON, Canada, in 2004.In 1998, he joined the Department of Computer Science and Technology, Peking University, Beijing, China. In 1999, he joined the Department of Electrical and Computer Engineering, McMaster University, where he worked as a postdoctoral fellow, a research associate, and a research engineer. Heis currently an Assistant Professor with the Department of Electrical and Electric Engineering, Southern University of Science and Technology, Shenzhen, China. His research interests include surrogate modeling, CAD, modeling of microwave circuits, software design technology, andmethodologies for microwave CAD.